

# Effects of grain boundary adhesion and grain size on ductility of thin metal films on polymer substrates

Zhao Zhang<sup>a</sup> and Teng Li<sup>a,b,\*</sup>

<sup>a</sup>Department of Mechanical Engineering, University of Maryland, College Park, MD 20742, USA

<sup>b</sup>Maryland NanoCenter, University of Maryland, College Park, MD 20742, USA

Received 28 May 2008; revised 20 June 2008; accepted 20 June 2008

Available online 15 July 2008

We have studied the effects of grain boundary adhesion and grain size on the ductility of thin metal films well bonded to polymer substrates, using a finite element method. It is shown that the ductility of polymer-supported metal films increases approximately linearly as the grain boundary adhesion increases, and as the grain size decreases. A rule-of-thumb estimate of the ductility of polymer-supported metal films agrees well with the simulation results.

© 2008 Acta Materialia Inc. Published by Elsevier Ltd. All rights reserved.

**Keywords:** Ductility; Thin metal films; Polymers; Nanocrystalline materials; Grain boundaries

There has been a surge of interest in developing flexible electronics for various applications, such as paper-like displays [1], flexible solar cells [2] and electronic skin [3]. Many such flexible devices consist of thin films of stiff materials (e.g. metals) on substrates of compliant materials (e.g. polymers). When stretched, the compliant substrate deforms, but the stiff films may fracture. For example, it has often been reported that thin metal films, freestanding or polymer-supported, rupture at small strains (<2%) [4–7]. Some recent experiments, however, demonstrate that metal films well bonded to polymer substrates can sustain large strains (up to 50%) [8–11]. The origins of the substantial variation in the ductility of thin metal films on polymer substrates remain unclear. This paper shows that the ductility of thin metal films well bonded to polymer substrates depends strongly on the grain boundary adhesion and the grain size of the metal films.

When stretched, a freestanding thin metal film can deform plastically. Upon further straining, the film does not harden as much as its bulk counterpart, as the dislocations in the film can readily escape from the free surfaces. Therefore, once film thinning occurs, further deformation is localized near the thinning region, leading to necking rupture. Since plastic deformation is vol-

ume-conserved, local thinning results in a local elongation comparable to the film thickness. Consequently, the rupture strain can be estimated by the thickness-to-length ratio of the film, which is usually extremely small.

When a metal film bonded to a polymer substrate is stretched, the local elongation of the film is constrained by the substrate. Such a constraint retards strain localization in the film, so that the metal film can deform uniformly to a large strain. For example, simulations show that a Cu film well adherent to a polyimide substrate should sustain strains exceeding 80% [12]. The ductility of polymer-supported metal films can be modulated by the metal/polymer interfacial adhesion [13]. Under a modest tension, a weakly adhered metal film can debond from the substrate; the film becomes freestanding and is free to form a neck, resulting in low ductility. Recent experiments with Cu films on polyimide substrates show that poorly bonded Cu films form channel cracks at strains ~2%, while well-bonded Cu films can sustain strains up to 10% without appreciable cracks [9].

While existing simulations predict extraordinary ductility of thin metal films well bonded to polymer substrates (e.g. >80%), the best reported experimental observation so far is up to 50%. Such a discrepancy between experiment and theory may result from assuming the metal films to be ductile continuum in existing simulations. Such an assumption limits the failure mode of the metal films to strain localization (e.g. necking). By contrast, experiments show that thin metal films well

\* Corresponding author. Address: Department of Mechanical Engineering, and Maryland NanoCenter, University of Maryland, College Park, MD 20742, USA; e-mail: [LiT@umd.edu](mailto:LiT@umd.edu)

bonded to polymer substrates fail by both local thinning and intergranular cracking [9]. If the grain boundaries in a metal film are brittle, intergranular cracking involves breaking a layer (or several layers, at most) of atomic bonds, thus requiring little additional space to proceed. As a result, the polymer substrate cannot effectively constrain intergranular cracking, resulting in low ductility of the metal film. On the other hand, if the grain boundaries are tough, intergranular fracture takes place when grain boundary crack opening exceeds a threshold value of finite magnitude. Such finite crack openings in the metal film require local space to accommodate, and thus are constrained by the polymer substrate. Accordingly, the metal film ruptures at a modest strain. Furthermore, the effect of grain boundary cracking on the ductility of polymer-supported thin metal films can be modulated by the grain size, given that more metal atoms are associated with grain boundaries as the grain size becomes smaller. The above considerations suggest that the grain boundary adhesion and the grain size play important roles in the ductility of thin metal films well bonded to polymer substrates.

The effects of grain boundary adhesion and grain size on the ductility of nanocrystalline metals have been intensively studied recently [14–19]. Most of these efforts, however, have investigated nanocrystalline metals in bulk and freestanding forms. As discussed above, the tensile behavior of polymer-supported metal films differs from that of freestanding metal films. So far, the effects of grain boundary adhesion and grain size on the ductility of polymer-supported thin metal films remain largely unexplored [20]. To address the above concern and plan further experiments, this paper studies such effects using a finite element method.

Figure 1 depicts the simulation model. Under tension, a thin blanket metal film well bonded to a thick polymer substrate is subject to grain boundary cracking (Fig. 1a). For simplification, the following assumptions are made: there is only one grain along the film thickness direction (e.g. a very thin metal film with columnar grains); all grains have the same size  $d$  along the tensile direction; the intergranular cracking occurs along grain boundaries perpendicular to the tensile direction (all other grain boundaries are not subject to cracking, and thus are not considered in the simulation). The limitations of the above assumptions will be discussed later in the paper. The metal/polymer laminate is taken to deform under plain strain conditions. Taking advantage of symmetry, we model only a unit cell of the laminate, consisting of two halves of adjacent grains, the grain boundary

in between and the substrate underneath (Fig. 1b). In the simulation model, the film is a layer of thickness  $h$ , and the substrate is a block of thickness  $100h$  and length  $d$ . The horizontal displacement is set to be zero along the centerline of the laminate, and set to be  $u/2$  along both sides of the laminate. The quantity  $u/d$  will be called the applied strain. A V-shaped notch,  $0.2h$  wide and  $0.02h$  deep, is placed at the top of the grain boundary to introduce an imperfection.

Both the metal grains and the polymer are modeled as elastic–plastic solids. Under uniaxial tension, the true stress  $\sigma$  and the natural strain  $\varepsilon$  follow the relation:

$$\sigma = \begin{cases} \sigma = E\varepsilon, & \varepsilon \leq \sigma_Y/E \\ \sigma_Y \left( \frac{\varepsilon}{\sigma_Y/E} \right)^N, & \varepsilon > \sigma_Y/E \end{cases} \quad (1)$$

where  $E$  is Young's modulus,  $N$  the hardening exponent, and  $\sigma_Y$  the yield strength. In the simulations, the following values are used:  $E = 100$  GPa,  $N = 0.02$  and  $\sigma_Y = 100$  MPa for the metal; and  $E = 8$  GPa,  $N = 0.5$  and  $\sigma_Y = 50$  MPa for the polymer.

As illustrated in Figure 2, the grain boundary is modeled as an array of nonlinear springs, characterized by a tensile and a shear traction–displacement law, with six parameters: interfacial tensile strength  $\sigma_n$  and shear strength  $\sigma_s$ , critical opening displacement  $\delta_n$  and sliding displacement  $\delta_s$ , and the areas under the traction–displacement curves  $\Gamma_n$  and  $\Gamma_s$  (i.e. the normal and shear fracture toughness of the grain boundary, respectively). The metal/polymer interface is also modeled as an array of nonlinear springs, with similar traction–displacement laws but with different values of parameters. We assume that  $\sigma_n = \sigma_s$ ,  $\delta_n = \delta_s$  and  $\Gamma_n = \Gamma_s$  for both the grain boundary and the metal/polymer interface. The grain boundary and the metal/polymer interface are meshed with four-node cohesive elements sharing nodes with the neighboring elements in the film and the substrate.

Given the focus on the intergranular cracking of thin metal films well bonded to polymer substrates, a strong metal/polymer interface is assumed (i.e.  $\sigma_{n,s} = 100$  MPa,  $\delta_{n,s} = 0.1$   $\mu\text{m}$ ,  $\Gamma_{n,s} = 5$  J/m<sup>2</sup>). With such a strong interface, no appreciable debonding occurs in all simulations. In the rest of the paper, we will use  $\sigma_{n,s}$ ,  $\delta_{n,s}$  and  $\Gamma_{n,s}$  to denote the parameters of the traction–displacement law for the grain boundary.

In describing the simulation results, we will use two types of dimensionless groups:  $h/d$  and  $\Gamma_{n,s}E_f/\sigma_{Y_f}^2h$ , where  $E_f$  and  $\sigma_{Y_f}$  are the Young's modulus and the yield stress of the metal, respectively. Various values of  $h/d$  (0.05–0.8) and  $\Gamma_{n,s}E_f/\sigma_{Y_f}^2h$  (10–230) are used to study

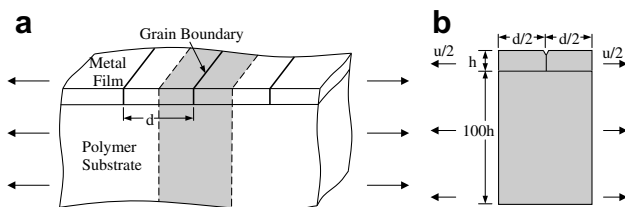


Figure 1. (a) Schematics of a blanket thin metal film on a polymer substrate, subject to tension. (b) The unit cell used in the simulation model (the shaded area in (a)).

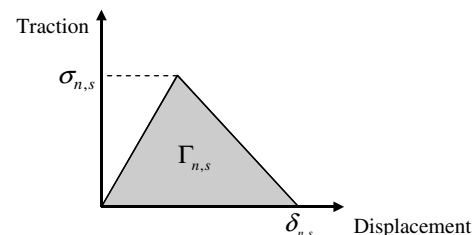


Figure 2. The traction–separation laws used to model the grain boundary and the metal/polymer interface.

the effect of grain size and grain boundary adhesion, respectively. Our simulations show that, once the grain boundary adhesion  $\Gamma_{n,s}$  is fixed, the values of  $\sigma_{n,s}$  and  $\delta_{n,s}$  are of secondary importance to the intergranular cracking. Consequently, we will not discuss our results in terms of  $\sigma_{n,s}$  and  $\delta_{n,s}$ .

Figure 3 shows the deformation sequence of a unit cell of the metal/polymer laminate. At small applied strains, the metal grains elongate and the grain boundary starts to open from the film surface. When the grain boundary opening exceeds  $\delta_{n,s}$ , intergranular cracking initiates (Fig. 3a). Further deformation in the metal film will be localized at the grain boundary while there is little further straining of the metal grains, as evident by the roughly similar stress levels in the metal grains at various applied strains. Under larger applied strains, the intergranular cracking propagates toward the metal/polymer interface (Fig. 3b). The rupture strain of the thin metal film,  $\epsilon_{cr}$ , is defined as the applied strain at which the intergranular cracking advances to a length of 80% of the film thickness  $h$  (Fig. 3c).

Figure 4a plots rupture strain  $\epsilon_{cr}$  as a function of normalized grain boundary adhesion  $\Gamma_{n,s}E_f/\sigma_Y^2h$  for various  $d/h$ . The rupture strain of the thin metal film increases as the grain boundary adhesion increases, in a roughly linear manner. For a given grain boundary adhesion, the rupture strain remains almost the same when  $d/h > 10$ , and increases as the grain size becomes smaller. Such an increase in rupture strain becomes substantial when  $d/h < 5$ . For example, for a polymer-supported metal film of 100 nm thick, with strong grain boundary adhesion  $\Gamma_{n,s} = 2.3 \text{ J/m}^2$  and grain size 120 nm, the predicted rupture strain is about 50%.

Figure 4b further elucidates the effect of the grain size on the rupture strain, by plotting  $\epsilon_{cr}$  as a function of  $h/d$  for various  $\Gamma_{n,s}E_f/\sigma_Y^2h$ . While the rupture strain slightly increases with decreasing grain size when  $h/d < 0.2$ , it increases almost linearly with  $1/d$  when  $h/d > 0.2$ , for various grain boundary adhesions.

The dependence of the rupture strain on the grain size in Figure 4b can be explained as follows. As shown in Figure 3, the strain in the metal grains remains approximately unchanged after intergranular cracking initiates and propagates along the grain boundary. Upon rupture, the net deformation of the metal film in a unit cell consists of two parts: the elongation of the metal grains and the opening of the grain boundary. Therefore, the

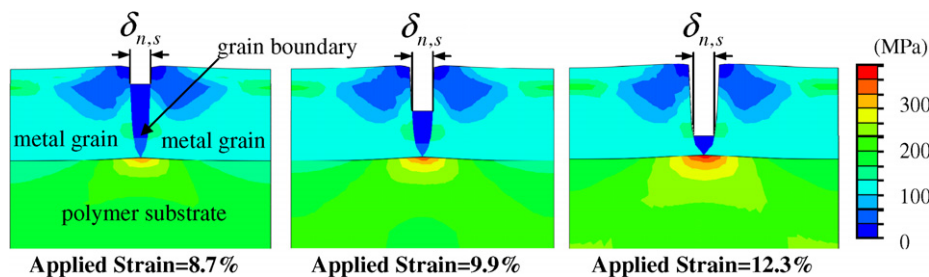


Figure 3. Deformation sequence of a unit cell of a metal/polymer laminate. Note the propagation of the grain boundary crack from the top surface to the metal/polymer interface. Only part of the substrate thickness is shown. Contour colors represent the von Mises stress level. Here,  $\Gamma_{n,s}E_f/\sigma_Y^2h = 110$ ,  $d/h = 2.6$ .

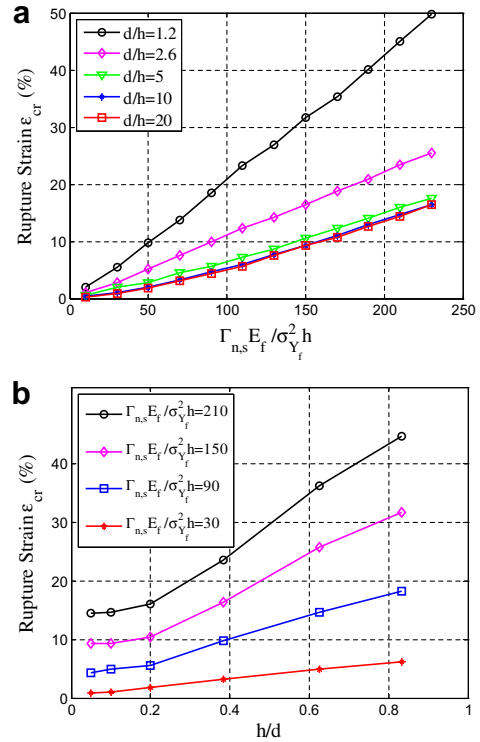


Figure 4. (a) Rupture strain as the function of grain boundary adhesion for various grain sizes. (b) Rupture strain as the function of grain size for various grain boundary adhesions.

rupture strain, estimated by the net deformation of the metal film divided by its length (i.e.  $d$  in the unit cell), is:

$$\epsilon_{cr} = \epsilon_N + \alpha \frac{\delta_{n,s}}{d}, \tag{2}$$

where  $\epsilon_N$  is strain level in the metal grains and  $\alpha$  is a dimensionless number of order unity. The value of  $\epsilon_N$  is approximately equal to the hardening index  $N$  for a weakly hardening metal. From Eq. (2), for a metal film with grain size much larger than its thickness, the rupture strain remains roughly as a constant level of  $\epsilon_N$ . By contrast, for a metal film with grain size comparable to its thickness, the second term in the right-hand side of Eq. (2) dominates, and the rupture strain is linearly proportional to  $1/d$ .

Figure 5 compares the estimated rupture strain from Eq. (2) with the simulation results. For example, taking

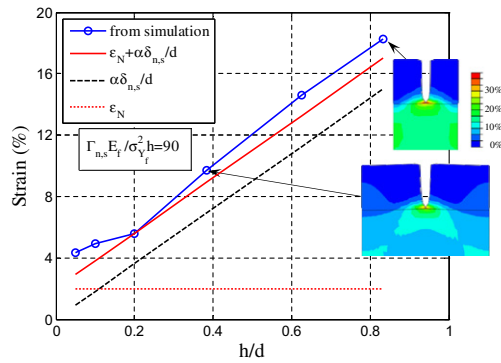


**Figure 5.** Comparison between the rupture strain from the simulations (circles) and the estimate from Eq. (2) (solid line), for various grain sizes. The insets show the deformed shapes of the unit cells at rupture for two grain sizes,  $h/d=0.38$  and  $0.83$ , respectively. Note the approximately similar strain level in the metal grains, although the applied strains are significantly different (9.7% and 18.2%, respectively). The contour shades represent the strain component in the tensile direction.

$\Gamma_{n,s}E_f/\sigma_y^2h = 90$ ,  $\epsilon_N = 0.02$ ,  $\delta_{n,s}/h = 0.18$  and  $\alpha = 1$ , the simple estimate of Eq. (2) agrees with the simulation results within 10% when  $h/d > 0.2$ . The insets of Figure 5 clearly show that, upon rupture, the strain level in the metal grains of different sizes remains approximately the same, comparable to the metal hardening index (i.e. 2%).

The present model assumes there is one grain along the film thickness direction and all grains have the same size along the tensile direction. Under such assumptions, all grain boundary cracks initiate from the film surface simultaneously. In practice, a thin metal film on a polymer substrate may have several grains along its thickness direction, and the size of the metal grains often varies. The random distribution of the metal grains leads to stress concentrations in certain locations in the metal film (e.g. triple junctions and missing grains). Furthermore, a real thin metal film on a polymer substrate often has non-uniform thickness due to interface and film surface roughness, and material texture. Recent experiments show that the metal/polymer interface and the metal free surface further roughen substantially under large tensile strains [21–23]. The rough interface and free surface can also result in stress concentrations in the metal film. The stress concentrations provide extra driving force for grain boundary cracking initiation and propagation. As stated above, the present model may overestimate the rupture strain of the metal films. On the other hand, the intergranular cracks in a real metal film are often locally zig-zag, even though the overall crack path is roughly perpendicular to the tensile direction. As a result, the total surface area of such a rough crack is larger than that of a smooth crack. In this sense, the present model may underestimate the rupture strain of the metal films. Further studies are needed to take into account the effects of non-uniform distribution of the metal grains (e.g. size and orientation), which will be reported elsewhere.

In summary, we use a finite element method to simulate the rupture process of thin metal films well bonded to polymer substrates due to grain boundary cracking. The simulation results delineate an approximately linear dependence of the metal film ductility on the grain boundary adhesion, as well as on the reciprocal of grain size for small grains. To achieve high ductility of metal films on polymer substrates, strong grain boundary adhesion and small grain size are desired. A rule-of-thumb estimate of the ductility of polymer-supported metal films is in good agreement with the simulation results. The present study sheds light on the underpinning mechanisms that govern the ductility of thin metal films on polymer substrates. We therefore call for further experiments to verify the results of the present study.

This work is supported by the Ralph E. Powe Jr. Faculty Award from Oak Ridge Associated Universities and by Minta-Martin Foundation. Z.Z. also acknowledges the support of an A.J. Clark Fellowship.

- [1] G.P. Crawford (Ed.), Flexible Flat Panel Displays, Wiley, New York, 2005.
- [2] C.J. Brabec, Sol. Energ. Mater. Sol. Cells 83 (2004) 273.
- [3] S. Wagner, S.P. Lacour, J. Jones, P.I. Hsu, J.C. Sturm, T. Li, Z. Suo, Physica E 25 (2005) 326.
- [4] D.W. Pashley, Proc. Roy. Soc. Lond. A 255 (1960) 218.
- [5] H. Huang, F. Spaepen, Acta Mater. 48 (2000) 3261.
- [6] S.L. Chiu, J. Leu, P.S. Ho, J. Appl. Phys. 76 (1994) 5136.
- [7] B.E. Alaca, M.T.A. Saif, H. Sehitoglu, Acta Mater. 50 (2002) 1197.
- [8] P. Gruber, J. Böhm, A. Wanner, L. Sauter, R. Spolenak, E. Arzt, Mater. Res. Soc. Symp. Proc. 821 (2003) P2.7.
- [9] Y. Xiang, T. Li, Z. Suo, J.J. Vlassak, Appl. Phys. Lett. 87 (2005) 161910.
- [10] R.M. Niu, G. Liu, C. Wang, G. Zhang, X.D. Ding, J. Sun, Appl. Phys. Lett. 90 (2007) 161907.
- [11] N. Lu, X. Wang, Z. Suo, J.J. Vlassak, Appl. Phys. Lett. 91 (2007) 221909.
- [12] T. Li, Z.Y. Huang, Z.C. Xi, S.P. Lacour, S. Wagner, Z. Suo, Mech. Mater. 37 (2005) 261.
- [13] T. Li, Z. Suo, Int. J. Solids Struct. 44 (2007) 1696.
- [14] M. Legros, B.R. Elliott, M.N. Rittner, J.R. Weertman, K.J. Hemker, Philos. Mag. A 80 (2000) 1017.
- [15] L. Lu, S.X. Li, K. Lu, Scr. Mater. 45 (2001) 1163.
- [16] Y.M. Wang, M. Chen, F. Zhou, E. Ma, Nature 419 (2002) 912.
- [17] Y.M. Wang, K. Wang, D. Pan, K. Lu, K.J. Hemker, E. Ma, Scr. Mater. 48 (2003) 1581.
- [18] M.A. Haque, M.T.A. Saif, Proc. Natl. Acad. Sci. USA 101 (2004) 6335.
- [19] M. Dao, L. Lu, R.J. Asaro, J.T.M. De Hosson, E. Ma, Acta Mater. 55 (2007) 4041.
- [20] N. Lu, X. Wang, Z. Suo, J.J. Vlassak, (2008), preprint: Available from: <<http://imechanica.org/node/3320>>.
- [21] O. Wouters, W.P. Vellinga, R. van Tijing, J.T.M. De Hosson, Acta Mater. 54 (2006) 2813.
- [22] R. van Tijing, W.P. Vellinga, J.T.M. De Hosson, Acta Mater. 55 (2007) 2757.
- [23] R. van Tijing, B.V.C. de Jong, W.P. Vellinga, J.T.M. De Hosson, Surf. Coat. Tech. 201 (2007) 4633.